



Ultrasound evidence for a two-component superconducting order parameter in Sr₂RuO₄

S. Benhabib^{1,11}, C. Lupien^{2,11}, I. Paul³✉, L. Berges¹, M. Dion², M. Nardone¹, A. Zitouni¹, Z. Q. Mao^{4,5}, Y. Maeno^{4,6}, A. Georges^{7,8,9,10}, L. Taillefer^{2,6}✉ and C. Proust^{1,6}✉

The quasi-two-dimensional metal Sr₂RuO₄ is one of the best characterized unconventional superconductors, yet the nature of its superconducting order parameter is still under debate^{1–3}. This information is crucial to determine the pairing mechanism of Cooper pairs. Here we use ultrasound velocity to probe the superconducting state of Sr₂RuO₄. This thermodynamic probe is sensitive to the symmetry of the material, and therefore, it can help in identifying the symmetry of the superconducting order parameter^{4,5}. Indeed, we observe a sharp jump in the shear elastic constant c_{66} as the temperature is increased across the superconducting transition. This directly implies that the superconducting order parameter is of a two-component nature. On the basis of symmetry arguments and given the other known properties of Sr₂RuO₄ (refs. 6–8), we discuss which states are compatible with this requirement and propose that the two-component order parameter $\{d_{xz}, d_{yz}\}$ is the most likely candidate.

In conventional superconductors, the pairing mechanism originates in the interaction of electrons with phonons, and the resulting superconducting order parameter has *s*-wave symmetry. As per the Fermi statistic, the orbital symmetric state of two electrons must combine with an antisymmetric spin-singlet part. In contrast, in superfluid ³He (where ferromagnetic spin fluctuations are the mechanism responsible for pairing), the resulting spin states are in the triplet state. In this case, the orbital part of two ³He atoms has *p*-wave symmetry⁹. For 25 years, the superconductivity of Sr₂RuO₄ has been viewed as an electronic analogue of superfluid ³He (refs. 1–3). The initial report of the temperature-independent spin susceptibility through the superconducting temperature T_c (ref. 10) and the indication of time-reversal symmetry breaking^{11,12} pointed to a spin-triplet, chiral, *p*-wave order parameter. However, several experiments have contradicted this scenario¹³, for example, the lack of edge currents¹⁴, the Pauli-limiting critical field¹⁵ and the absence of a cusp in the dependence of T_c on uniaxial strain¹⁶. Importantly, the evidence of line nodes in the gap from specific heat¹⁷, ultrasound attenuation¹⁸ and thermal conductivity^{6,19} is not compatible with a chiral *p*-wave order parameter because it has no symmetry-imposed node for a two-dimensional Fermi surface. Recently, measurements of the NMR Knight shift were carefully revisited, and a clear drop in the spin susceptibility below T_c was detected⁷, pointing to an order parameter with even parity. As a result, the chiral *p*-wave order

parameter is excluded and the nature of the superconducting state in Sr₂RuO₄ is now a wide open question.

Sound velocity is a powerful thermodynamic probe for the order parameter. For propagation along high-symmetry directions of the crystal, the sound velocity is $v_s = \sqrt{\frac{c_{ij}}{\rho}}$, where ρ is the density of the material and c_{ij} are the elastic constants in the Voigt notation defined as the second derivative of the free energy F with respect to the strain u_{ij} . Within the framework of the Landau–Ginzburg theory of phase transitions, the observation of a discontinuity in the elastic constant at the superconducting transition is a consequence of the symmetry-allowed coupling term between the order parameter Δ and strain u , which takes the form $\lambda|\Delta|^2u$, where λ is the coupling constant²⁰. As part of the free energy, this coupling term is invariant under all the operations of the point group, meaning that it belongs to the A_{1g} representation. Table 1 lists the irreducible strains corresponding to the point group D_{4h} for the tetragonal symmetry of Sr₂RuO₄ (see the corresponding product table in Supplementary Section 6). If the superconducting order parameter has one component, then $|\Delta|^2$ belongs to the A_{1g} representation. Consequently, the strain variable u can only belong to the A_{1g} representation; therefore, it corresponds to a longitudinal sound wave. A jump in the longitudinal elastic constant is observed at T_c in many superconductors and is directly related to the jump in the specific heat at T_c and the strain dependence of T_c via the Ehrenfest relation⁴. If an unusual jump in the elastic constant associated with a shear mode (B_{1g} or B_{2g} representation) is detected at T_c , then it necessarily implies that the superconducting order parameter has more than one component^{4,5,21}.

On the basis of these symmetry arguments that are further developed in this paper, we have performed the measurements of longitudinal and transverse sound velocities in Sr₂RuO₄ across the superconducting transition down to 40 mK. The initial measurements²² have been confirmed only recently using a different spectrometer (Supplementary Section 2) and by a complementary technique²³.

Table 2 lists the different acoustic modes along with the directions of sound propagation and polarization of the transducer. The value of the sound velocity is obtained from the echo spacing at a low temperature ($T=4$ K) and can be converted to elastic constants using $\rho=5.95$ g cm⁻³. These values are in good agreement with the resonant ultrasound spectroscopy measurements^{23–25}. Figure 1a,b shows the

¹Laboratoire National des Champs Magnétiques Intenses (CNRS, EMFL, INSA, UGA, UPS), Toulouse, France. ²Institut Quantique, Département de physique & RQMP, Université de Sherbrooke, Sherbrooke, Québec, Canada. ³Laboratoire Matériaux et Phénomènes Quantiques, Université de Paris, CNRS, Paris, France. ⁴Department of Physics, Kyoto University, Kyoto, Japan. ⁵Department of Physics, The Pennsylvania State University, University Park, PA, USA. ⁶CIFAR, Toronto, Ontario, Canada. ⁷Collège de France, Paris, France. ⁸Center for Computational Quantum Physics, Flatiron Institute, New York, NY, USA. ⁹CPHT, Ecole Polytechnique, CNRS, Université Paris-Saclay, Palaiseau, France. ¹⁰Department of Quantum Matter Physics, University of Geneva, Geneva, Switzerland. ¹¹These authors contributed equally: S. Benhabib, C. Lupien. ✉e-mail: indranil.paul@univ-paris-diderot.fr; louis.taillefer@usherbrooke.ca; cyril.proust@lncmi.cnrs.fr

Table 1 | Irreducible representations Γ of the D_{4h} point group in terms of the components of wavevector k and the strain tensor u_{ij} . a and b are constants

Γ	Basis function	Strain component	Elastic constant
A_{1g}	$a(k_x^2 + k_y^2) + bk_z^2$	$u_{xx} + u_{yy}, u_{zz}$	$(c_{11} + c_{12})/2, c_{33}$
A_{2g}	$k_x k_y (k_x^2 - k_y^2)$	None	None
B_{1g}	$k_x^2 - k_y^2$	$u_{xx} - u_{yy}$	$(c_{11} - c_{12})/2$
B_{2g}	$k_x k_y$	u_{xy}	c_{66}
E_g	$k_x k_z, k_y k_z$	u_{xz}, u_{yz}	c_{44}

Table 2 | Definition of the different sound modes measured at $T = 4$ K

Elastic constant	k	p	Sound velocity (km s ⁻¹)	Value (GPa)
c_{11}	[100]	[100]	6.28	233
c_{44}	[100]	[001]	3.41	68.2
c_{66}	[100]	[010]	3.3	64.3
$(c_{11} - c_{12})/2$	[110]	[1 $\bar{1}$ 0]	2.94	51

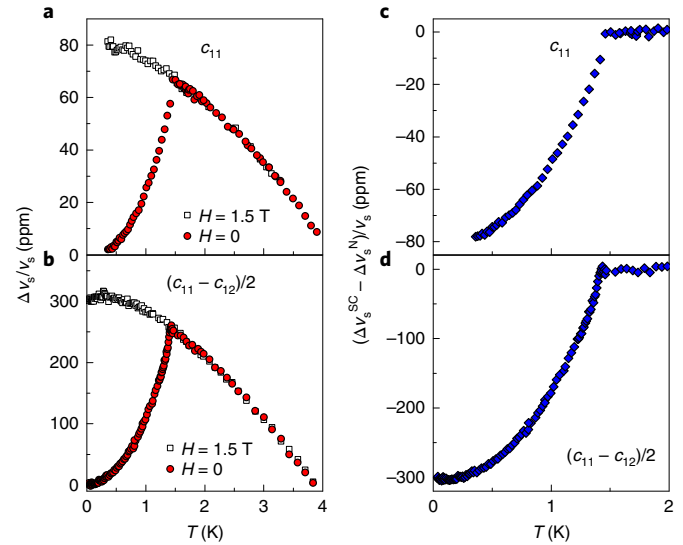
k and p denote the propagation and polarization directions, respectively. Sound velocities were obtained at a low temperature using echo spacing.

temperature dependence of the sound velocity for the longitudinal mode c_{11} and the transverse mode $(c_{11} - c_{12})/2$, respectively. The red circles (open squares) correspond to measurements in the superconducting (normal) state. Figure 1c,d shows the difference between the superconducting and normal states for the two modes. A discontinuity is expected at T_c for the longitudinal mode c_{11} . We estimate the magnitude of this drop to be $\Delta c_{11}/c_{11} \approx 2$ ppm. This rough estimation is based on the Ehrenfest relation that links the jump in the sound velocity with the jump in the specific heat and the strain dependence of T_c (Supplementary Section 3). This small discontinuity at T_c is, therefore, hidden by the strong softening in the longitudinal constant in the superconducting state (approximately 80 ppm between T_c and $T=0$). Similar, but even stronger, softening is observed for the transverse mode of $(c_{11} - c_{12})/2$ below T_c (Fig. 1b). These results are qualitatively in agreement with previous measurements^{26,27}, but the absolute value of their elastic constants differs from ours, although more recent measurements have clarified this situation.

Figure 2a shows the temperature dependence of the sound velocity for the transverse mode c_{66} . The measurements in the superconducting state ($H=0$; red circles) display a sharp discontinuity at the superconducting transition. The difference in the shear sound velocity between the normal and superconducting states (Fig. 2b) shows a small but clear jump at T_c , of a magnitude of approximately 0.2 ppm, which is ten times larger than our experimental resolution. The exceptional sensitivity of our experiment is due to the very small attenuation of the c_{66} mode¹⁸, which enabled us to detect up to approximately 60 echoes (Supplementary Fig. 1) and to perform a fit on all of them.

Note that if there is any mixing of acoustic modes in the measurement, the small jump in c_{66} can easily be swamped by the huge softening of the other modes. In a second experiment, using a different spectrometer, we were able to again detect the sharp drop below T_c in Sr_2RuO_4 , but with some contamination from the other modes (Supplementary Fig. 2). In the data shown in Fig. 2b, the complete lack of any temperature dependence below 1.3 K down to 0.04 K is evidence against such contamination.

This is the key finding of our study: we observe a sharp discontinuity at T_c in the sound velocity for the transverse mode c_{66} . This

**Fig. 1 | Relative change in the sound velocity of Sr_2RuO_4 through T_c .**

a, b. Temperature dependence of the sound velocity for the longitudinal mode of c_{11} measured at $f=83$ MHz (**a**) and the transverse mode of $(c_{11} - c_{12})/2$ measured at $f=21.5$ MHz (**b**). Data for the normal state (open squares) are obtained by applying a magnetic field H of 1.5 T in the plane, which is larger than the upper critical field H_{c2} . Data for the superconducting state (red circles) are measured without any applied field. **c.** Difference between the superconducting (SC) and normal (N) states for the c_{11} mode. **d.** Difference between the superconducting and normal states for the $(c_{11} - c_{12})/2$ mode.

immediately provides good evidence that the superconducting order parameter must be of a two-component nature, consistent only with the E_g singlet representation, E_u triplet representation or an accidentally degenerate combination of two one-dimensional representations.

A discontinuity in the sound velocity in the c_{66} mode at T_c of approximately 10 ppm was recently detected in Sr_2RuO_4 by resonant ultrasound spectroscopy performed at frequency $f \approx 2$ MHz (ref. ²³). The difference in the magnitude of the jump may come from a finite-frequency effect on the dynamics of the order parameter. The consequence is a decrease in the amplitude of the anomaly as the frequency increases (Supplementary Section 4 and ref. ⁴). Note that a rough estimation of the magnitude of the c_{66} drop using the Ehrenfest relation is about 2 ppm (Supplementary Section 3).

Now, we discuss the Landau theory describing the strain-order parameter coupling. Sr_2RuO_4 displays D_{4h} symmetry, and only the irreducible representation, E , of the point group is multi-dimensional. In this representation, the superconducting order parameter is a two-component complex variable (Δ_A, Δ_B) . If the order parameter has E_u symmetry, (Δ_A, Δ_B) transforms into (x, y) ; if the order parameter has E_g symmetry, it transforms into (xz, yz) . For both cases, the Landau–Ginzburg free energy describing Δ and uniform strain u is given by

$$F = F_\Delta + F_u + F_{\Delta-u}. \quad (1)$$

The superconducting part, expanded to the fourth order, is

$$F_\Delta = a(|\Delta_A|^2 + |\Delta_B|^2) + \beta_1^0(|\Delta_A|^2 + |\Delta_B|^2)^2 + \frac{\beta_2^0}{2}[(\Delta_A^*)^2 \Delta_B^2 + \text{c.c.}] + \beta_3^0|\Delta_A|^2|\Delta_B|^2.$$

Here $a=0$ at the superconducting transition, β are constants, and c.c. implies complex conjugation. The relevant elastic energy of the uniform strain is

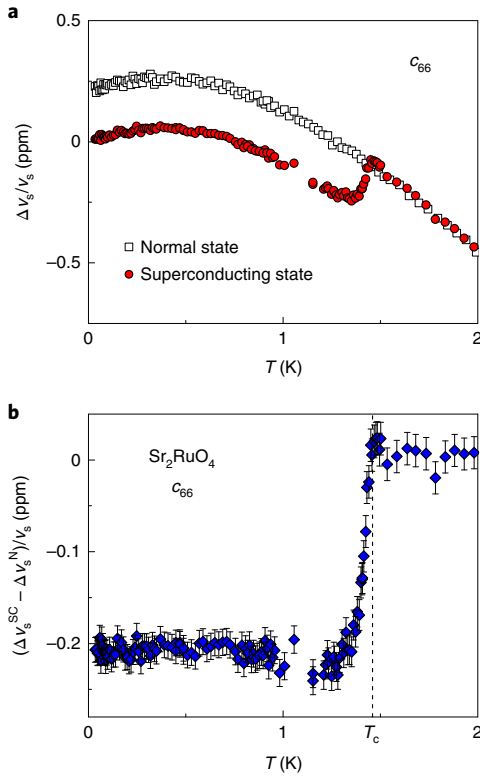


Fig. 2 | Jump in the c_{66} shear modulus at T_c . **a**, Relative change in the sound velocity for the transverse mode c_{66} measured at $f = 169$ MHz. Data for the normal state (open squares) are obtained by applying a field of 1.5 T in the plane. Data for the superconducting state (red circles) are measured without any applied field. **b**, Difference between the superconducting and normal states for the c_{66} mode. A clear, discontinuous jump is observed at T_c . The error bars are estimated from the constant-voltage noise on the echoes measured by using the phase comparator.

$$F_u = \frac{1}{2} c_{11} (u_{xx}^2 + u_{yy}^2) + c_{12} u_{xx} u_{yy} + 2c_{66} u_{xy}^2 + \frac{1}{2} c_{33} u_{zz}^2 + c_{13} (u_{xx} + u_{yy}) u_{zz},$$

where c denote elastic constants in the Voigt notation. The cross-coupling term is

$$F_{\Delta-u} = [\alpha_1 (u_{xx} + u_{yy}) + \alpha_2 u_{zz}] (|\Delta_A|^2 + |\Delta_B|^2) + \alpha_3 (u_{xx} - u_{yy}) (|\Delta_A|^2 - |\Delta_B|^2) + \alpha_4 u_{xy} (\Delta_A^* \Delta_B + \text{c.c.}).$$

Here, α are coupling constants. The analysis of the above free energy is standard, and it is described in detail in Supplementary Section 7. Similar expressions for the chiral p -wave state have been calculated by other groups^{4,5,21}. Here we quote the main results.

For convenience, we define $c_A \equiv (c_{11} + c_{12})/2$ and $c_O \equiv (c_{11} - c_{12})/2$. The latter is the orthorhombic elastic constant associated with the shear mode $u_{xx} - u_{yy}$, while c_{66} is the elastic constant of the monoclinic shear u_{xy} . Our aim is to calculate the jumps in the shear elastic constants defined by $\delta c \equiv c(T_c^-) - c(T_c^+)$.

The term $F_{\Delta-u}$ renormalizes the fourth-order coefficients $\beta_i^0 \rightarrow \beta_i$ with

$$\begin{aligned} \beta_1 &= \beta_1^0 - \frac{1}{2} \left[\frac{\alpha_2^2}{c_O} + \frac{\alpha_1^2 c_{33} + \alpha_2^2 c_A - 2\alpha_1 \alpha_2 c_{13}}{c_A c_{33} - c_{13}^2} \right], \\ \beta_2 &= \beta_2^0 - \alpha_4^2 / (4c_{66}), \\ \beta_3 &= \beta_3^0 - \alpha_4^2 / (4c_{66}) + 2\alpha_3^2 / c_O. \end{aligned}$$

For the stability of the system, we need $\beta_1 > 0$ and $4\beta_1 \pm \beta_2 + \beta_3 > 0$. Within these ranges, the following three superconducting phases are possible.

Case (1): time-reversal-symmetry-broken superconductor. In the region $\beta_2 > (0, \beta_3)$, we get the time-reversal-symmetry-broken state with $(\Delta_A, \Delta_B) = \Delta_0(1, \pm i)$. In this phase, there is no spontaneous shear strain and the tetragonal symmetry is preserved. The shear moduli jumps are

$$\delta c_{66} = \frac{-\alpha_4^2}{4\beta_2 + \alpha_4^2/c_{66}}, \quad (2a)$$

$$\delta c_O = \frac{-2\alpha_3^2}{\beta_2 - \beta_3 + 2\alpha_3^2/c_O}. \quad (2b)$$

Case (2): nematic–monoclinic superconductor. In the region $\beta_2 < (0, -\beta_3)$, we get a nematic solution, namely, $(\Delta_A, \Delta_B) = \Delta_0(1, \pm 1)$, which breaks the tetragonal symmetry by making the two in-plane diagonal directions inequivalent. It is accompanied by a spontaneous monoclinic strain, that is, $u_{xy} \neq 0$. The shear moduli jumps are

$$\delta c_{66} = \frac{-\alpha_4^2/2}{4\beta_1 + \beta_2 + \beta_3 + \alpha_4^2/(2c_{66})}, \quad (3a)$$

$$\delta c_O = \frac{-2\alpha_3^2}{|\beta_2| - \beta_3 + 2\alpha_3^2/c_O}. \quad (3b)$$

Case (3): nematic–orthorhombic superconductor. In the region $\beta_3 > (0, |\beta_2|)$, we also get a nematic solution, namely, $(\Delta_A, \Delta_B) = \Delta_0(0, 1)$ or equivalently $\Delta_0(1, 0)$, which also breaks the tetragonal symmetry by making the two in-plane crystallographic axes inequivalent. It is accompanied by spontaneous orthorhombic strain such that $u_{xx} - u_{yy} \neq 0$. The shear moduli jumps are

$$\delta c_{66} = \frac{-\alpha_4^2/2}{\beta_2 + \beta_3 + \alpha_4^2/(2c_{66})}, \quad (4a)$$

$$\delta c_O = \frac{-\alpha_3^2}{2\beta_1 + \alpha_3^2/c_O}. \quad (4b)$$

Thus, in all the three states, the two shear elastic constants, c_{66} and c_O , jump at T_c . In our data, there is a clear jump in c_{66} . However, a jump in c_O could not be resolved, most likely because of the strong temperature dependence of $c_O(T)$ below the transition.

The observed jump in c_{66} at T_c implies that the superconducting order parameter of Sr_2RuO_4 has a two-component characteristic. Now, we discuss the various implications of this new constraint in the context of the other known properties of Sr_2RuO_4 .

(1) Discrete symmetry breaking: in a two-component scenario, the $U(1)$ -symmetry-breaking superconducting transition is necessarily accompanied by simultaneous discrete symmetry breaking. For case (1), this discrete symmetry involves time reversal leading to spontaneous magnetization that can be detected in muon spin relaxation (μSR) measurements. For example, a non-zero μSR signal below T_c has indeed been reported¹¹, but its origin and implications are currently under investigation²⁸. For cases (2) and (3), the broken symmetry is tetragonal D_4 leading to monoclinic or orthorhombic distortion in the tetragonal unit cell, respectively. In principle, it can be detected through X-ray diffraction, but no such distortion has been reported yet.

(2) Response to uniaxial pressure: T_c as a function of the B_{1g} shear strain $u_{xx} - u_{yy}$ is expected to increase linearly. However, experimentally, T_c increases quadratically with the uniaxial strain ϵ_{100} along [100], and therefore, the cusp at zero strain has not been observed. Note that due to the Poisson effect, ϵ_{100} is a combination of $u_{xx} - u_{yy}$ and the in-plane A_{1g} longitudinal strain $u_{xx} + u_{yy}$. This implies that

at the quadratic order in ϵ_{100} , there is B_{1g} perturbation that should lead to the splitting of the superconducting transition if the order parameter is of the (1, i) or (1, 1) type (Supplementary Section 8). However, for (1, 0), one expects a single transition, with enhanced T_c . Since specific heat measurements detect no splitting of the superconducting transition under the application of strain (at least along the [100] direction)⁸, the behaviour of Sr_2RuO_4 under uniaxial pressure argues in favour of the (1, 0) order parameter. (Here we assume that the strain-independent transition observed recently by zero-field μSR ²⁸ is not related to the superconducting state.)

(3) Spin-wave-vector content of Cooper pairs: the drop in the Knight shift below T_c is strongly suggestive of an even-parity order parameter^{7,29}. Assuming only intraband pairing, for singlets, the lowest harmonic is a d -wave solution, that is, $(\Delta_A, \Delta_B) = \Delta_0(k_x k_z, k_y k_z)$. For triplets, to be consistent with recent NMR as well as polarized neutron scattering data³⁰, the lowest-harmonic, triplet order parameter is the p -wave solution $(\Delta_A, \Delta_B) = \Delta_0 k_z (\hat{d}_x, \hat{d}_y)$.

(4) Line nodes: experimentally, thermal conductivity measurements show that the gap has vertical line nodes⁶. Whether the gap can also have horizontal line nodes is a quantitative question (Supplementary Section 5). Recent data from quasiparticle interference experiments can be interpreted in terms of vertical line nodes along the diagonal³¹, as that in the $d_{x^2-y^2}$ state. Data regarding the variation in specific heat as a function of the angle of an in-plane magnetic field relative to the crystal have been interpreted either in terms of vertical line nodes of the $k_x k_z$ type³² (that is, rotated by 45° compared with the $d_{x^2-y^2}$ state) or the horizontal line nodes³³. All the states that we discuss within the E_g and E_u representations necessarily have horizontal line nodes. In the singlet sector (E_g), the states (1, 0) and (1, 1), which break tetragonal symmetry, also have vertical line nodes (respectively in the [100] and [110] directions). However, the state (1, i), which breaks time-reversal symmetry, typically does not have vertical line nodes, unless the pairing leads to a Bogoliubov Fermi surface³⁴. In the triplet sector (E_u), the p -wave solutions do not have vertical line nodes. To have triplet solutions that are consistent with the vertical line nodes, one needs to consider a higher harmonic f -wave solution, namely, $(\Delta_A, \Delta_B) = \Delta_0 k_z (k_x^2 - k_y^2) (\hat{d}_x, \hat{d}_y)$.

(5) Accidental degeneracy: until now, we only considered the two-dimensional irreducible representation E. In principle, one can also get two-dimensional Δ if two one-dimensional representations become accidentally degenerate. The advantage of such a scenario is that it allows the possibility of having a finite jump in c_{66} while having no jump in c_{10} . Thus, the ($s+d$)-wave solution, $(\Delta_A, \Delta_B) = (1, k_x k_y)$, will have the same free energy structure as that in equation (1), except for $\alpha_3 = 0$. However, such a state is not guaranteed to have line nodes. Vertical line nodes are present for accidental degeneracy of higher-order harmonics such as the ($d+g$)-wave solution $(\Delta_A, \Delta_B) = (k_x^2 - k_y^2) (1, k_x k_y)$ ³⁵.

If we combine the following arguments, namely, (1) the superconducting order parameter has two components; (2) the gap has vertical line nodes (from thermal conductivity⁶); (3) the order parameter has even parity (from NMR⁷); and (4) uniaxial strain does not split the superconducting transition (from specific heat under strain⁸); and if we disregard the evidence of time-reversal symmetry breaking^{11,12,28}, then the only possible candidate is the (1, 0) state in the E_g representation, namely, the nematic state $k_x k_z$ (or $k_y k_z$), with both horizontal and vertical line nodes. The onset of this nematic state is accompanied by an orthorhombic distortion in the lattice, as well as the formation of nematic domains. These structural changes should be detectable by X-ray diffraction measurements.

Online content

Any methods, additional references, Nature Research reporting summaries, source data, extended data, supplementary information, acknowledgements, peer review information; details of author contributions and competing interests; and statements of

data and code availability are available at <https://doi.org/10.1038/s41567-020-1033-3>.

Received: 28 February 2020; Accepted: 7 August 2020;
Published online: 21 September 2020

References

- Maeno, Y. et al. Superconductivity in a layered perovskite without copper. *Nature* **372**, 532–534 (1994).
- Rice, T. M. & Sigrist, M. Sr_2RuO_4 : an electronic analog of ^3He ? *Phys. Condens. Matter* **7**, L643–L648 (1995).
- Mackenzie, A. P. & Maeno, Y. The superconductivity of Sr_2RuO_4 and the physics of spin-triplet pairing. *Rev. Mod. Phys.* **75**, 657–712 (2003).
- Sigrist, M. Ehrenfest relations for ultrasound absorption in Sr_2RuO_4 . *Prog. Theor. Phys.* **107**, 917–925 (2002).
- Walker, M. B. & Contreras, P. Theory of elastic properties of Sr_2RuO_4 at the superconducting transition temperature. *Phys. Rev. B* **66**, 214508 (2002).
- Hassinger, E. et al. Vertical line nodes in the superconducting gap structure of Sr_2RuO_4 . *Phys. Rev. X* **7**, 011032 (2017).
- Pustogow, A. et al. Constraints on the superconducting order parameter in Sr_2RuO_4 from oxygen-17 nuclear magnetic resonance. *Nature* **574**, 72–75 (2019).
- Li, Y. S. et al. High sensitivity heat capacity measurements on Sr_2RuO_4 under uniaxial pressure. Preprint at <https://arxiv.org/abs/1906.07597> (2019).
- Legett, A. J. A theoretical description of the new phases of liquid ^3He . *Rev. Mod. Phys.* **47**, 331–414 (1975).
- Ishida, K. et al. Spin-triplet superconductivity in Sr_2RuO_4 identified by ^{17}O Knight shift. *Nature* **396**, 658–660 (1998).
- Luke, G. M. et al. Time-reversal symmetry-breaking superconductivity in Sr_2RuO_4 . *Nature* **394**, 558–561 (1998).
- Xia, J. et al. High resolution polar Kerr effect measurements of Sr_2RuO_4 : evidence for broken time-reversal symmetry in the superconducting state. *Phys. Rev. Lett.* **97**, 167002 (2006).
- Mackenzie, A. P. et al. Even odder after twenty-three years: the superconducting order parameter puzzle of Sr_2RuO_4 . *npj Quantum Mater.* **2**, 40 (2017).
- Kirtley, J. R. et al. Upper limit on spontaneous supercurrents in Sr_2RuO_4 . *Phys. Rev. B* **76**, 014526 (2007).
- Deguchi, K. et al. Superconducting double transition and the upper critical field limit of Sr_2RuO_4 in parallel magnetic fields. *J. Phys. Soc. Jpn* **71**, 2839–2842 (2002).
- Hicks, C. W. et al. Strong increase of T_c of Sr_2RuO_4 under both tensile and compressive strain. *Science* **344**, 283–285 (2014).
- Nishizaki, S., Maeno, Y. & Mao, Z. Q. Changes in the superconducting state of Sr_2RuO_4 under magnetic fields probed by specific heat. *J. Phys. Soc. Jpn* **69**, 572–578 (2000).
- Lupien, C. et al. Ultrasound attenuation in Sr_2RuO_4 : an angle-resolved study of the superconducting gap function. *Phys. Rev. Lett.* **86**, 5986–5989 (2001).
- Suzuki, M. et al. Universal heat transport in Sr_2RuO_4 . *Phys. Rev. Lett.* **88**, 227004 (2002).
- Rehwald, W. The study of structural phase transitions by means of ultrasonic experiments. *Adv. Phys.* **22**, 721–755 (1973).
- Contreras, P. et al. Symmetry field breaking effects in Sr_2RuO_4 . *Rev. Mex. Fis.* **62**, 442–449 (2016).
- Lupien, C. *Ultrasound Attenuation in the Unconventional Superconductor Sr_2RuO_4* . PhD thesis, Univ. Toronto (2002).
- Ghosh, S. et al. Thermodynamic evidence for a two-component superconducting order parameter in Sr_2RuO_4 . *Nat. Phys.* <https://doi.org/10.1038/s41567-020-1032-4> (2020).
- J.P. Paglione et al. Elastic tensor of Sr_2RuO_4 . *Phys. Rev. B* **65**, 220506 (2002).
- Barber, M. E. et al. Role of correlations in determining the van Hove strain in Sr_2RuO_4 . *Phys. Rev. B* **100**, 245139 (2019).
- Matsui, H. et al. Ultrasonic studies of the spin-triplet order parameter and the collective mode in Sr_2RuO_4 . *Phys. Rev. B* **63**, 060505R (2001).
- Okuda, N. et al. Unconventional strain dependence of superconductivity in spin-triplet superconductor Sr_2RuO_4 . *J. Phys. Soc. Jpn* **71**, 1134–1139 (2002).
- Grinenko, V. et al. Split superconducting and time-reversal symmetry-breaking transitions, and magnetic order in Sr_2RuO_4 under uniaxial stress. Preprint at <https://arxiv.org/abs/2001.08152> (2020).
- Ishida, K., Manago, M. & Maeno, Y. Reduction of the ^{17}O Knight shift in the superconducting state and the heat-up effect by NMR pulses on Sr_2RuO_4 . *J. Phys. Soc. Jpn* **89**, 034712 (2020).
- Petsch, A. N. et al. Reduction of the spin susceptibility in the superconducting state of Sr_2RuO_4 observed by polarized neutron scattering. Preprint at <https://arxiv.org/abs/2002.02856> (2020).
- Sharma, R. et al. Momentum-resolved superconducting energy gaps of Sr_2RuO_4 from quasiparticle interference imaging. *Proc. Natl Acad. Sci. USA* **10**, 5222–5227 (2020).

32. Deguchi, K. et al. Gap structure of the spin-triplet superconductor Sr_2RuO_4 determined from the field-orientation dependence of the specific heat. *Phys. Rev. Lett.* **92**, 047002 (2004).
33. Kittaka, S. et al. Searching for gap zeros in Sr_2RuO_4 via field-angle-dependent specific-heat measurement. *J. Phys. Soc. Jpn* **87**, 093703 (2018).
34. Suh, H. G. et al. Stabilizing even-parity chiral superconductivity in Sr_2RuO_4 . *Phys. Rev. Res.* **2**, 032023 (2020).
35. Kivelson, S. A. et al. A proposal for reconciling diverse experiments on the superconducting state in Sr_2RuO_4 . *npj Quantum Mater.* **5**, 43 (2020).

Publisher's note Springer Nature remains neutral with regard to jurisdictional claims in published maps and institutional affiliations.

© The Author(s), under exclusive licence to Springer Nature Limited 2020

Methods

Samples. Our experiments were carried out on two oriented pieces cut from a single high-quality crystal of Sr_2RuO_4 grown by the travelling-solvent floating-zone technique³⁶. T_c is defined as the peak of the magnetic susceptibility and is 1.4 K. The samples were polished to 1 μm roughness, with two opposite faces whose parallelism was estimated to be better than 1.5 $\mu\text{m mm}^{-1}$. The alignment of the polished faces relative to the crystal axes was determined by using the Laue back-reflection method and it was off-axis by less than 0.5° for the measurements shown in the main text. One sample was aligned with the polished face perpendicular to (100) and the other sample was perpendicular to (110).

Ultrasound measurements. The measurements were performed with a pulse-echo technique using two home-built spectrometers and commercial LiNbO_3 transducers. Most of the measurements were performed in a dilution refrigerator in Toronto³⁷ (by C.L. and C.P. in the Taillefer lab), with the transducer bonded to the crystals with a thin layer of an optical coupling compound (Dow Corning 20-057).

The amplitude and phase were measured using a phase comparator between a reference signal and the signal from the sample. The outputs of the phase comparator, in-phase I and quadrature Q , give the amplitude of the signal $A = \sqrt{I^2 + Q^2}$ and phase $\phi = \arctan(Q/I)$.

The c_{66} mode was later re-investigated in a separate experiment—performed in Toulouse—using another spectrometer, in a ^3He refrigerator with the transducer bonded to the crystals with AngstromBond glue (AB9110). In this case, the amplitude of the signal was measured using a logarithmic amplifier. The phase was measured using a phase comparator, but with a limiting amplifier at the input, to have perfect decoupling between the phase and amplitude of the signal.

In the reflective configuration (using only one transducer), the sound wave propagates forward along the sample and is reflected by the parallel, opposite face; further, it hits the same transducer again. Supplementary Figure 1 shows an example of the amplitude of the signal for the c_{66} mode measured in Toronto. Each forward-and-back travel of the sound wave corresponds to one echo; up to 60 echoes were detected. The variation in the sound velocity is given by

$$\frac{\Delta v_s}{v_s} = \frac{1}{\omega} \frac{\partial \phi}{\partial t} \quad (5)$$

where $\omega = 2\pi f$ and f is the frequency of the measurement. Since the phase is linearly increasing with time t , we can perform a linear fit to the phase of different echoes versus time. By using all the echoes in a weighted fit, the noise is reduced; further, the sensitivity of the measurement is close to 0.02 ppm.

Data availability

All data that support the findings of this study are available from the corresponding authors on request.

References

36. Mao, Z. Q., Maeno, Y. & Fukazawa, H. Crystal growth of Sr_2RuO_4 . *Mater. Res. Bull.* **35**, 1813–1824 (2000).

Acknowledgements

We thank J. Chang, J.C. Davis, C. Kallin, S.A. Kivelson, D. LeBoeuf, W.A. MacFarlane, A.P. Mackenzie, V. Madhavan, B.J. Ramshaw, G. Rikken, M. Sigrist, D. Vignolles and M.B. Walker for helpful and stimulating discussions. Part of this work, associated with the PhD thesis of C.L. working with C.P. under the supervision of L.T., was performed at the University of Toronto. C.P. acknowledges support from the EUR grant NanoX no. ANR-17-EURE-0009 and from the ANR grant NEPTUN no. ANR-19-CE30-0019-01. L.T. acknowledges support from the Canadian Institute for Advanced Research (CIFAR) as a CIFAR Fellow and funding from the Natural Sciences and Engineering Research Council of Canada (NSERC; PIN: 123817), the Fonds de recherche du Québec—Nature et Technologies (FRQNT), the Canada Foundation for Innovation (CFI) and a Canada Research Chair. This research was undertaken thanks in part to funding from the Canada First Research Excellence Fund. Y.M. acknowledges support from JSPS Kakenhi (grants JP15H5852, JP15K21717 and JP17H06136) and the JSPS-EPSCRC Core-to-Core Program of Oxide Superspin (OSS). A.G. acknowledges the support of the European Research Council (ERC-319286-QMAC). The Flatiron Institute is a division of the Simons Foundation.

Author contributions

C.L. and C.P. performed the ultrasound measurements in Toronto. S.B., L.B. and C.P. performed the ultrasound measurements in Toulouse. S.B., C.L., L.B., M.D. and C.P. analysed the data. I.P. performed the calculations, with input from A.G. M.N. and A.Z. conceived and realized the ^3He cryostat in Toulouse. Z.Q.M. and Y.M. prepared and characterized the Sr_2RuO_4 sample. I.P., L.T. and C.P. wrote the manuscript in consultation with all the authors. I.P., L.T. and C.P. co-supervised the project.

Competing interests

The authors declare no competing interests.

Additional information

Supplementary information is available for this paper at <https://doi.org/10.1038/s41567-020-1033-3>.

Correspondence and requests for materials should be addressed to I.P., L.T. or C.P.

Reprints and permissions information is available at www.nature.com/reprints.